Cytotoxicity of fractured quartz on human macrophages: role of the membranolytic activity of quartz and phagolysosome destabilization.

Riccardo Leinardi
Universita degli Studi di Torino Dipartimento di Chimica https://orcid.org/0000-0002-2570-3568
Cristina Pavan
Universite Catholique de Louvain
Harita Yedavally
Rijksuniversiteit Groningen
Maura Tomatis
Universita degli Studi di Torino Dipartimento di Chimica
Anna Salvati (a.salvati@rug.nl)
Rijksuniversiteit Groningen
Francesco Turci (francesco.turci@unito.it)
University of Torino https://orcid.org/0000-0002-5806-829X

Research

Keywords: Quartz, surface, cytotoxicity, membrane, phagolysosome

Posted Date: April 2nd, 2020

DOI: https://doi.org/10.21203/rs.3.rs-20378/v1

Abstract

Background The pathogenicity of quartz involves lysosomal alteration in alveolar macrophages. This event triggers the inflammatory cascade that may lead to quartz-induced silicosis and eventually lung cancer. Recently, we showed that synthetic quartz induces membrane lysis in red blood cells and cytotoxic responses in murine alveolar macrophages, only when the atomic order of crystal surfaces is upset by fracturing. Cytotoxicity was not observed when quartz exhibited as-grown, unfractured surfaces. These findings raised questions on the potential impact of quartz surfaces on the phagolysosomal membrane upon internalization of the particles by macrophages.

Results To gain insights on the surface-induced cytotoxicity of quartz, as-grown and fractured quartz particles in respirable size, differing only in surface properties related to fracturing, were prepared and physico-chemically characterized. Their effects were compared to a well-known toxic commercial quartz dust. Membranolysis was assessed on red blood cells, and quartz uptake, cell viability, and impact on lysosomes were assessed on human PMA-differentiated THP-1 macrophages. All quartz samples were internalized, but only fractured quartz elicited cytotoxicity and phagolysosomal alterations. These effects were blunted when uptake was suppressed. Membranolysis, but not cytotoxicity, was quenched when fractured quartz surface was masked with serum proteins and incubated with cells.

Conclusions Upon internalization, the phagolysosome environment rapidly removes serum proteins from quartz surface, restoring quartz membranolytic activity in the phagolysosomes. Fractured quartz induces cytotoxicity in THP-1 human macrophages by promoting phagolysosomal membrane alterations.

Background

Exposure to crystalline silica dusts, in particular quartz, induces severe toxic effects in humans [1–3]. It is also known that a cluster of dust properties, including particle size [4, 5], the capacity to induce free radicals [6–8], and the degree of hydrophilicity, related to the distribution of siloxanes and silanol families on the particle surface [9, 10], give a contribution to the adverse effects of quartz in vitro and in vivo. The various adverse cellular effects reported in the literature are related to particle-membrane interactions [11], and to the activation of lung cells [12–14]. Recently, a revisited mechanism of toxicity for quartz particles in the alveolar space has been proposed [15]. According to this model, inhaled particles are recognized and internalized by alveolar macrophages to be cleared out from the lungs [16]. The deposition of non-cleared particles onto the alveolar epithelium causes the recruitment and the activation of new macrophages and neutrophils, in a self-sustained detrimental process which gives rise to persistent inflammation, as long as the particles remain in the alveolar space.

The alveolar macrophages (AM) are among the first cells of the body to have significant contact with inhaled particles [16]. Because of the active phagocytosis of AM, quartz particles mainly interact with the macrophage phagolysosomal membrane [17]. It is in fact known that most particles accumulate at

lysosomal level following uptake, and because of this, the particle impact on the phagolysosomes is a key parameter to be investigated [18–22].

Upon quartz phagocytosis, lysosome membrane permeabilization (LMP) may occur and, the lysosomal content, such as cathepsins B and S [21, 23], may leak into the cytosol. As recently evidenced, this event can trigger the NALP3 inflammasome machinery [23, 24], which in turn causes activation of the proteolytic enzyme caspase-1 and the release of active pro-inflammatory cytokines (i.e. IL-1β and IL-18) [25, 26].

The interaction of quartz particles with the phagolysosomal membrane, a crucial step according to the model of quartz-induced inflammogenicity, was recently proposed as the molecular initiating event (MIE) of the quartz adverse outcome pathway (AOP) towards persistent inflammation and silicosis [15]. In search for the molecular determinant of this interaction, a considerable number of works have been published in the last few years [26–29]. Traditionally, a well-established biomembrane model is represented by the red blood cell [30], and hemolysis is largely used to probe the interaction of amorphous and crystalline silica particles with biomembranes [27, 31, 32]. Recently, we have demonstrated that synthetic quartz crystals are hemolytic only upon mechanical fracturing, a procedure that upsets the expected long-range order of quartz non-radical surface moieties (such as silanols, silanolates, siloxanes) [28]. In previous studies, several approaches were developed to modulate cellular responses to quartz, by modifying its surface in many different ways [33–35]. However, a clear connection between the surface states and features of different quartz particles and their impact on cellular membranes, and more particularly the phagolysosomal membrane, still needs to be established.

Here, we investigate the impact of quartz particles on human macrophages, specifically analyzing whether quartz can induce alterations of the phagolysosome membrane. To this aim, we compared the effect on cell viability and impact at lysosomal level of three surface-differentiated quartz specimens, namely: an ad-hoc synthesized quartz crystal in respirable size [36], exposing as-grown, unfractured, regular faces; a synthetic quartz mechanically fractured down to a size similar to the as-grown quartz; and a cytotoxic commercial quartz dust used in several toxicological works, as a positive control [37–40]. Human red blood cells were used as model of cellular membrane (not capable of internalization) for assessing quartz membranolytic activity, and for evidencing the effect of protein adsorption on the membranolytic activity of fractured quartz. PMA-differentiated THP-1 monocytes were selected as a common model for human alveolar macrophages [41–43]. Particle uptake was monitored by TEM and a combination of cell viability and flow cytometry-based assays was used to determine alterations induced at lysosomal level. This work provides novel and fundamental insights on the mechanisms of the pathogenicity of quartz, clarifying the nature of the molecular initiating event resulting from the interaction of quartz crystals with the phagolysosomes, following particle internalization by macrophages.

Results

As-grown and fractured crystals share similar physico-chemical properties

To study the impact of quartz particles on phagolysosome membrane, two synthetic quartz samples, with as-grown regular (gQ) or fractured (gQ-f) surfaces were prepared, from a similar synthesis [36]. A commercial quartz dust (cQ-f) was used as positive control, due to its known ability to induce cytotoxicity, increase in lysosomal permeability, and inflammogenic activity [44–47]. Overall, physico-chemical characterization results showed that samples share both particle size distribution and, albeit to a lesser extent, surface charge, under the test conditions (Table 1).

Table 1 - Main physico-chemical properties of the investigated samples

le	Origin	Surface state	FPIA Size[a](mm ±s.d.)	DLS diameter[b](mm±s.d.) (PDI)	SSA[c](m^2/g)	ζ-potential (mV±s.d.)		
						s.f. RPMI[d]	cRPMI[e]	0.01 NaCl[f]
	synthetic	as-grown	1.3±2.3	0.89±0.23 (0.507)	5.8	ca. 0	-11±1	-45±2
	synthetic	fractured	1.2±0.7	1.55±0.18 (0.485)	4.5	ca. 0	-12±1	-50±1
	commercial	fractured	1.0±1.2	1.74±0.20 (0.295)	4.3	ca. 0	-10±1	-59±2

a. Measured by flow particle image analyser (FPIA) in ultrapure H_2O.

b. Measured by dynamic light scattering (DLS) in +RPMI + 10% FBS, the polydispersity index (PDI) is reported in brackets.

c. Measured by Kr-BET method.

d. Measured by electrophoretic light scattering (ELS) in serum free RPMI (pH ca. 8)

e. Measured by electrophoretic light scattering (ELS) in RPMI + 10% FBS (pH ca. 8)

f. Measured by electrophoretic light scattering (ELS) in 0.01 M NaCl (pH 4.5)

Dimensional characterization showed that the samples had respirable micrometric size. FE-SEM analysis confirmed that as-grown gQ crystals had a well-organized morphology, with flat and smooth surfaces. Fractured gQ-f and cQ-f exhibited a morphology typical of industrial quartz dust, (Figure 1), as previously evidenced [48].

Specific surface area (SSA, Kr-BET) and particle size distribution (dynamic light scattering, DLS, and flow particle image analysis, FPIA) of the synthetic samples were comparable with the positive control quartz

(Table 1). The SSA of gQ-f was slightly lower than that of gQ, because the latter contains a slightly larger fraction of fine particles, as evidenced by the DLS analysis.

The zeta potential of particles (ELS, measured in various medium at specific pH), here used to describe the average acidity of surface silanols [29], acidic moieties with a potential for H-bonding, showed no significant differences among the set of samples, for the same medium. As expected, the zeta potential of particles dispersed in saline (0.01 M NaCl) at pH 4.5, which represents the lysosomal pH, was strongly negative (< -40 mV). Only small differences among zeta potential, namely gQ being less negatively charged than gQ-f and cQ-f, were detected, due to the different surface silanol population of as-grown and fractured crystals, confirming previous findings [28]. Such a difference was not observed when particles were dispersed in serum free RPMI, where all samples exhibited a zeta potential close to the point of zero charge (pzc). The measure of the zeta potential was also used to evaluate the adsorption of serum proteins on the quartz surface [49]. Upon dispersion of particles in RPMI supplemented with 10% FBS, all quartz samples exhibited a negative zeta potential (ca. -10 mV), compatible with the adsorption of serum proteins on the particle surface and the formation of the protein corona.

As-grown and fractured crystals are both internalized by human macrophages

The uptake and cytotoxicity of the different quartz particles were evaluated on PMA-differentiated THP-1 human monocytes, here chosen as a common model for human alveolar macrophages [41–43]. Transmission electron microscopy (TEM) of thin cross-sections of quartz-incubated and fixated cells indicated that all the samples were internalized by the macrophages to the same extent (Figure 2), confirming previous finding in murine macrophages [28].

To take into account the hardness and particle dimension of quartz, sections were necessarily prepared with a larger thickness than conventional bio-TEM sections. No evidence of particles absorbed on the outer cell membrane was found. Inside the cells, both single particles and micrometric aggregates could be visualized. Due to the larger thickness of the sections and also the high density of the particles with respect to the cellular background, it was not clear whether the internalized particles were enclosed in vesicles, as expected following some form of endocytosis (Fig. 2d, 2f and 2h show details at higher magnification). In addition, section thickness impaired the observation of lysosomes, which usually are easy to recognize as darker organelles inside cells by TEM.

Exposure to fractured quartz reduces cell viability and induces phagolysosomal alterations

The impact of quartz on macrophage metabolic activity upon 24 h exposure to increasing doses of the different quartz particles was investigated by the MTT assay in complete medium. In addition, since particle uptake is usually followed by trafficking of the internalized materials to the lysosomes [18–22], we checked whether alterations at phagolysosomal level could be detected. The acidic compartment of macrophages exposed to quartz was stained (Figure 3) with the acidotropic probe Lyso Tracker Red [21].

Lyso Tracker staining is often used to detect lysosomal alterations [21, 50]; an increase in its intensity upon treatment is a sign of an increase in acidity of the lysosomal compartment or increase in number or volume of lysosomes. Loss of Lyso Tracker staining can instead be sign of lysosomal membrane permeabilization or a consequence of cell death.

Cells exposed to as-grown crystals (gQ) did not show any significant metabolic (Fig. 3a) or phagolysosomal alteration, even at the highest dose (Fig. 3b). On the contrary, exposure to fractured synthetic crystals (gQ-f) induced a considerable reduction of cell metabolic activity (Fig. 3a) and strong increase in Lyso Tracker intensity (Fig. 3b). In particular, the impact on phagolysosomes was appreciable already at low particle dosage, with a clear dose-response trend and effects similar to what observed with cQ-f quartz. The flow cytometry analysis also revealed a cellular sub-population with loss of Lyso Tracker staining at higher doses (Fig. 3c, orange curves, corresponding to particle concentration of 100 µg/ml), in particular in the case of cells treated with fractured quartz dusts (gQ-f and cQ-f), possibly due to dying cells. This is largely consistent with the cytotoxicity observed in the same conditions (Fig. 3a). Overall, these results clearly indicated that fractured quartz dusts induced decrease in cell metabolic activity and strong alterations of the acidic compartment of THP-1 macrophages.

Fractured quartz cytotoxicity is quenched when phagocytosis is prevented

To investigate whether cytotoxicity was induced via interactions at the outer cell membrane level or following particle internalization, the MTT and Lyso Tracker Red assays were repeated in energy depleted conditions, in order to suppress active uptake processes [18]. Cells were exposed for 4 hours to quartz in standard (37 °C / 4h) or energy-depleted (4 °C / 4h) conditions, then washed to remove extracellular particles, and incubated at 37 °C for 20 h, prior to MTT assay and Lyso Tracker staining (Figure 4).

The cytotoxicity and phagolysosome alterations resulting after 37 °C / 4h + 37 °C / 20h exposure (Fig. 4a and 4c) were similar to what observed after the conventional incubation (37 °C / 24h exposure, Fig. 3). On the contrary, cytotoxicity and phagolysosome alterations were almost completely suppressed when uptake was impaired (4 °C / 4h + 37 °C / 20h, Fig. 4b and 4d), indicating that both cellular responses are induced by fractured quartz only upon active internalization by THP-1 macrophages.

Hemolytic activity but not cytotoxicity is suppressed when surface of fractured quartz is coated with FBS proteins

To gain insights whether the interaction of quartz particles with membranes is modulated by the presence of biomolecules, we compared the effect of quartz dust in the presence and absence of foetal bovine serum proteins (FBS), as source of proteins. When quartz dusts come into contact with the lung lining fluid, the formation of a biomolecule layer, in particular proteins, possibly covering the surface of quartz is expected. To give evidence of the formation of the protein-coating, the surface charge of quartz dust incubated with FBS was assessed. The shift in zeta-potential of ca. – 10 mV (see Tab. 1) confirms the formation of a protein corona on FBS-incubated quartz. The capacity of the fractured synthetic sample

(gQ-f) to induce hemolysis was assessed by exposing RBCs to particles in the presence of increasing concentrations of FBS (Figure 5).

Importantly, FBS markedly reduced the hemolytic activity of fractured crystals. This effect was observed already at the lowest concentration of FBS and attained a complete suppression of the hemolytic activity at 0.3%. To investigate the role of particle surface in quartz cytotoxicity, we exposed THP-1 macrophages to the quartz samples in presence of 10% FBS in the medium (+ FBS) or in serum-free medium (- FBS). Cytotoxicity was assessed after 4 and 24 h by MTT assay (Figure 6a and 6b), and after 4 h by PI assay (Fig. 6c), used here as an additional marker of cytotoxicity.

The overall cytotoxicity, as expected, increased upon the incubation with fractured crystals. The cellular metabolic activity of the cells, assessed by MTT assay, significantly decreased after 4 and 24 h incubation time. Interestingly, at both exposure times (4 and 24 hours), a similar cell viability was observed when cells were exposed to fractured quartz dusts in medium with proteins or serum free medium. The PI assay further confirmed that only fractured quartz is cytotoxic, and allowed us to evidence a small but significant difference in % of PI positive cells when macrophages were exposed in + FBS or - FBS media.

Discussion

The permeabilization of the lysosomal membrane can lead to the intracellular inflammasome activation and release of pro-inflammatory mediators (IL-8, IL-1β) [17, 25, 51, 52, 53]. These events are observed upon prolonged exposure to respirable crystalline silica (RCS) and are held responsible for the induction of the persistent lung inflammation resulting, in the long term, in severe pathological outcomes, including lung cancer [54].

Previous research proposed the interaction of quartz with the phagolysosomal membrane to be the molecular initiating event (MIE) of the adverse outcome pathway (AOP) for quartz-induced lung pathologies [15]. In this work, we investigate the effects of quartz dusts on THP-1 monocytes PMA-differentiated into macrophages, chosen as a model for alveolar macrophages, and we focus on quartz impact on the phagolysosomal membrane. To understand how quartz initiates the inflammatory process in macrophages, we measured the membranolytic activity, the cytotoxicity, and the impact on phagolysosomes elicited by the surface-differentiated quartz crystals. The modulation of these readouts by serum proteins adsorbed on the surface of quartz was also determined, and allowed to propose an uptake-dependent mechanism of action for quartz in macrophages.

Quartz crystals with fractured surfaces, both synthetic and industrially produced, show a higher membranolytic activity than as-grown quartz dust suggesting that they might be able to induce a stronger destabilization of the macrophage membranes. Our data also indicate that all quartz dusts are internalized by THP-1 cell to a similar extent, but only quartz with fractured surfaces affects cell viability and induce lysosome alterations and cell death. Such a different behaviour of rather similar specimens can be explained with the differences in surface chemistry between as-grown and fractured crystals,

specifically due to the randomly distribution of surface functionalities (silanols and siloxanes) induced by mechanical fracturing [15, 28]. Interestingly, the impairment of active uptake obtained with the pre-incubation of cell and quartz at 4° C, suppresses the cytotoxic effects observed for fractured samples, including lysosomal alterations. The reduction of cytotoxicity in energy-depleted cells indeed suggests that the toxic activity of quartz is elicited after internalization by macrophages, confirming a direct action of the fractured quartz particle surface on the phagolysosomal membrane, rather than on the outer cell membrane. A further proof that the detrimental quartz-membrane interactions take place primarily at phagolysosomal level is given by the results obtained upon incubation of quartz with serum proteins (FBS). The suppression of the membranolytic activity when fractured quartz and RBCs are contacted in a FBS medium supports the hypothesis that serum proteins mask the surface reactive groups responsible for quartz membranolytic activity. This is in agreement with previous results [26, 45, 55], and corroborates what observed with other organic polymers [56–58]. Intriguingly, the protein coating on fractured quartz, evidenced by the change in surface charge, did not modify the cell viability impact towards THP-1 macrophages at 4 and 24 h (Fig. 4). These results suggest for a rapid removal of the protein coating after quartz is trafficked in the lysosomes, where likely the lysosomal acidity and lytic enzymes can restore the pristine surfaces of quartz as well as its membranolytic activity, thus in turn its pro-inflammatory action. This is also supported by the results of PI assay, in which the slightly lower cytotoxicity of protein-coated fractured particles, in comparison to what observed in serum-free media, suggests for an initial cleaning phase of quartz surfaces inside the phagolysosome, not yet completed at the shorter exposure time. The low surface area of quartz (ca. 5 m^2/g) accounts for this relatively rapid, yet biochemically similar, process in comparison to what has been previously evidenced for some nanoparticles accumulating in the phagolysosomes [21].

Overall, our data confirm that: i) quartz with fractured surfaces induce cytotoxicity and phagolysosomal alterations in human macrophages; ii) the quartz cytotoxic activity on THP-1 macrophages is dependent on particle uptake; and iii) the cytotoxic activity of quartz relies on direct interactions of fractured quartz surfaces with the phagolysosomal membrane.

The loss of long-range order surface moieties (silanols and siloxanes) induced by fracturing of regular crystals, macroscopically evidenced by the appearance of the typical conchoidal fractures of quartz [48], is here confirmed to be a key physico-chemical parameter in the toxicity of crystalline silica. In addition, we have gained new insights on the molecular initiating event (MIE) of quartz inflammatory mechanisms [15], as we observed that the detrimental effect of quartz is induced only when quartz particles are internalized, possibly when the phagolysosomal membrane is directly interacting with fractured quartz surfaces.

The molecular mechanisms leading to the observed alterations remain to be investigated. However, the results presented here support the hypothesis that quartz particles, after being internalized and cleaned up from adsorbed extracellular molecules in the phagolysosomes, may induce lysosomal membrane permeabilization [45]. Since the activation of NALP-3 inflammasome by quartz particles requires lysosome membrane damage [59], our results suggest that the surface chemistry of quartz crystals may

directly determine membrane destabilization, starting the well-described inflammatory process related to quartz pathological outcomes. The results obtained with this work confirm the improved model mechanism for quartz toxicity on human macrophages [15, 26, 28], and advance our knowledge on the alterations induced by fractured quartz on the phagolysosomal membrane, that are responsible for the initiation of quartz inflammogenic effect [45].

Conclusions

One of the most robust paradigm about the origin of the toxicological response to quartz dust involves the interaction of particles internalized by macrophages with the phagolysosomal membrane as the molecular initiating event (MIE) of quartz-induced cytotoxic and inflammatory response [15]. In the present work, we have observed that the internalization of quartz crystals by THP-1 macrophages resulted in cytotoxic effects, including a strong impact at lysosomal level, only when quartz is fractured. Cytotoxicity was quenched when the phagocytic activity of macrophages was prevented. In parallel, we observed that FBS suppressed the membranolytic activity, but not cytotoxicity, of fractured quartz, suggesting that quartz membrane lysis takes place in the phagolysosomes, following removal of proteins adsorbed on the particle surface. This led us to conclude that the interactions of the fractured crystal surfaces with the inner side of the phagolysosomal membrane, leading to its destabilization, are likely the cause of the observed impact on cell viability. On a broader level, this work suggests that toxic surface features of quartz could be predicted by a molecular knowledge of the surface chemistry of the dust. New investigations are currently being carried out to unveil the chemical nature of the surface features responsible for the membranolytic and cytotoxic activity of quartz [60, 61].

Methods

Crystalline silica samples

Two synthetic α-quartz samples with as-grown (gQ) or fractured (gQ-f) faces were used in this study. A commercial fractured α-quartz dust, largely used in studies of experimental silicosis and lung cancer (Min-U-Sil 5 quartz, US Silica Co., Berkeley Springs, WV, USA, lot number 15062696, in this work named cQ-f), was used as positive control.

Synthetic quartz crystals with as-grown regular faces (gQ) were obtained following the procedure developed by Pastero and coworkers [36]. Briefly, a 25% w/w Na-metasilicate (Na-MTS) solution was polymerized into a gel by the addition of 1 M HNO_3. The gel was stabilized at pH ≈ 8. Growth runs were performed in PTFE liner steel autoclaves at 210 °C, for 168 h. The finest fraction (< 30 mm), obtained through 30 minutes of sieving in 100 and 30 mm sieves, was used in all the experiments.

To obtain crystals with fractured faces (gQ-f), a further synthesis was carried out, where the Na-MTS solution was polymerized by bubbling CO_2 until gel formation, at pH ca. 8. The largest fraction (> 30 mm), obtained as above, was mechanically fractured by milling in a MM 200 mixer mill (Retsch, Haan,

Germany) in agate jars (27 Hz, two spheres, 500 mg of dust/jar) for 6 hours, in order to induce surface alterations.

Particle size distribution

Particle size distribution was determined by Flow Particles Image Analyzer (FPIA), using a Sysmex FPIA 3000 particle size and shape analyser (Malvern Panalytical, Malvern, UK) and by dynamic light scattering (DLS), using a Zetasizer Nano ZS (Malvern Instruments, Malvern, UK). For FPIA analysis, a sample dispersion of 0.5 mg/ml in MilliQ water was prepared and probe sonicated on ice for 3 minutes at 30% amplitude, power 25 W, using a Sonopuls HD3100 homogeniser (Bandelin, Berlin, Germany). For DLS analysis, a sample dispersion in RPMI medium (0.5 mg/ml), with the addition of 10% FBS, was prepared and sonicated as described.

Surface area determination

Specific surface area (SSA) was evaluated by the Brunauer-Emmett-Teller (BET) method, based on Kr adsorption. Quartz samples were firstly outgassed for two hours, at 150 °C. The analysis was then performed at -196 °C using an ASAP 2020 physisorption analyser (Micromeritics, Norcross, USA).

ζ-Potential

The ζ potential of the quartz samples was evaluated by means of electrophoretic light scattering (ELS) with a Zetasizer Nano–ZS (Malvern-Panalytical, Malvern, UK). In this technique, the velocity of a particle in an oscillating electric field, which is proportional to its ζ potential, is measured by light scattering. The ζ potential was measured after suspending quartz (0.5 mg/ml) in serum free RPMI medium or RPMI + 10% FBS, to evaluate the surface charge at exposure conditions (pH ca. 8) and the modulation given by serum proteins. Investigation of zeta potential at lysosomal pH (pH 4.5) was measured suspending quartz particles (0.5 mg/ml) in 0.01 M NaCl, and adjusting the pH of the suspension to the experimental value with 0.1 M HCl or 0.1 M NaOH.

Cell culture and THP-1 differentiation

RPMI 1640, FBS and DPBS were purchased from Gibco (Thermo Fischer Scientific, Waltham, MA, USA). Experiments were performed on human THP-1, a human monocyte-like cell line derived from a patient with leukaemia (ATCC#TIB-202) [62]. Cells suspensions were cultured in RPMI 1640 supplemented with 10% FBS (complete medium, cRPMI), at 37 °C and 5% CO_2. Just before seeding, (200000 or 100000 cells/well in a Cellstar 24-well plate for LysoTracker staining and PI staining, respectively, or 50000/well in a Cellstar transparent 96-well plate for MTT assay) cells were differentiated into macrophages by incubation with 100 nM PMA (phorbol 12-myristate 13-acetate) in cell culture medium for 48 h, at 37 °C and 5% CO_2 [63]. Transparent 24-well and 96-well plates were purchased from Greiner Bio-One (Kremsmunster, Austria).

TEM imaging

Particle uptake by THP-1 macrophages was investigated by means of transmission electron microscopy on cross sections of fixed cells, upon 24 h incubation with 50 µg/ml of synthetic or commercial quartz samples. After exposure, the cells were fixed with 0.2% glutaraldehyde and 2% PFA in 0.1 M sodium cacodylate buffer (pH 7.4) for 1 h. Then, cells were rinsed twice for 5 min in 0.1 M cacodylate buffer at room temperature followed by post-fixation in 1% osmium tetroxide/1.5% potassium ferrocyanide in 0.1 M sodium cacodylate at 4 °C for 30 min. The cells were then washed with Milli-Q water, dehydrated through serial incubation in a graded ethanol series (30, 50, 70 and 100%), and lastly embedded in EPON resin and polymerized at 37 °C for 16 h followed by 58 °C for 24 h. Given the size of the particles and the fact that they are hard to cut with a standard diamond knife, sections were cut at a thickness of 200 nm instead of the standard 80 nm using an UC7 ultramicrotome (Leica, Vienna, Austria). This allowed to partially reduce the presence of holes in the section, corresponding to areas were particles accumulate and that cannot be sectioned, while still being able to determine whether particle uptake was present. Sections were then contrasted using 5% uranyl acetate for 20 min, followed by Reynolds lead citrate for 2 min. Images were recorded with a CM100 Biotwin transmission electron microscope (FEI, Eindhoven, The Netherlands) operated at 80 KV using a Morada digital camera.

MTT assay

Cell metabolic activity was assessed through a MTT (3-(4,5-dimethylthiazol-2-yl)-2,5-diphenyltetrazolium bromide)) assay [64]. After differentiation, THP-1 macrophages, previously plated at a density of 50000 cells/well in a transparent 96-well plate, were exposed for 24 h to quartz particles at increasing concentrations (10, 25, 50, 100, 250 µg/ml) in complete medium (cRPMI, RPMI medium + 10% FBS). Before the assay, each well was washed with Dulbecco's Phosphate-Buffered Saline (DPBS) to remove the extracellular particles and eventual cell debris and treated with MTT (0.5 mg/ml) in cRPMI for 20 minutes at 37 °C. Then, MTT reagent was discarded and DMSO (200 µl) was added to each well, to solubilise formazan crystals. Each well was pipetted again to mix, and absorbance at 550 nm was measured using a THERMOmax microplate reader (Molecular Devices, San Josè, CA, USA). All values were normalized to the results obtained in untreated cells.

MTT assay was also carried out after 4 h of exposure at 4 °C, in order to block active cellular processes [65,66]. Plates with cells were pre-incubated at 4 °C for 30 minutes, just before the exposure to quartz particles (25, 50, 100, 250 µg/ml) in cRPMI. After 4 h of incubation, wells were washed three times with cRPMI (100 µl), and further incubated in fresh medium without particles for 20 h at 37 °C and 5% CO_2. The same protocol was applied for the 4-hours exposure, at 37 °C.

To assess protein modulation on quartz cytotoxicity, the MTT assay was carried out as previously explained, exposing PMA-differentiated THP-1 cells (50000 cells/well) for 4 or 24 h to quartz samples (100 mg/ml), in serum-free RPMI or RPMI supplemented with 10% FBS. The analysis was carried out as described above.

Lyso Tracker staining and flow cytometry

The impact on the lysosome after interaction and internalization of particles was investigated by staining cells with Lyso Tracker Red DND-99 (Thermo Fisher Scientific, Waltham, MA, USA), a fluorescent acidotropic probe for labelling and tracking acidic organelles in live cells. Increase in Lyso Tracker intensity from basal condition can be due to an increase in lysosomal volume, lysosomal number, or lysosomal acidity. THP-1 cells differentiated into macrophages were exposed to particle dispersions (25, 50, 100 mg/ml) prepared by diluting a stock dispersion (1 mg/ml) in cRPMI. Cells were grown on transparent 24-well plates (200000 cells/well) and exposed to particles 48 h after seeding. After 24 h exposure, at 37 °C and 5% CO_2, wells were washed (1x500 ml with complete medium) to remove quartz particles, then cells were incubated 15 minutes at 37 °C, 5% CO_2, with a solution (25 nmol, 500 ml) of Lyso Tracker Red DND-99 (Thermo Fisher Scientific, Waltham, MA, USA), in cRPMI. Then, the dye solution was discarded and wells were washed again with cRPMI (1x500 ml) and DPBS (2x500 ml). Cells were detached with 0.05% trypsin/EDTA (300 ml) at 37 °C for 5 minutes, followed by a treatment with EDTA solution (5 mmol) in PBS (pH 7.4), at 37 °C. Then, cells were harvested in FACS tubes and pelleted by centrifugation at 250g for 3 minutes. Cells were resuspended in DPBS (100 ml) and analysed using a CytoFlex flow cytometer (Beckman-Coulter, Brea, CA, USA). LysoTracker Red fluorescence intensity was analyzed in FL3 channel. Quantitative analysis of flow cytometry data was carried out using the FlowJo software (Tree Star, USA). Gates were set in order to discriminate cell debris and cell doublets from the analysis, according to their forward and side scattering. 20000 cells were acquired, unless specified in the case of samples for which strong cytotoxicity was detected (in these cases a variable number of cells, ranging from 20000 to at least ca. 7000 was acquired, as specified in figure captions). The same experiment was performed after 4 hours exposure at 4 and 37 °C, for cells exposed to 50 and 100 µg/ml of particles. The exposure at 4° C was preceded by a 30-minutes pre-incubation step of cells, at the same temperature.

Propidium iodide (PI) assay

THP-1 cells differentiated into macrophages were seeded on transparent 24-well plates (100000 cells/well) and, 48 h after seeding, cells were exposed to particles (final concentration: 100 mg/ml) in serum free (- FBS) or complete RPMI (+ FBS). After 4 h exposure at 37 °C and 5% CO_2, quartz dispersions were discarded and wells were washed with cRPMI (1x500 ml). Then, cells were harvested as described, collected into FACS tubes and stained with a PI solution (5 µg/ml) at room temperature. After incubation with the dye (15 minutes, 37° C), samples were measured as described above. A variable number of cells, ranging from 12000 to ca. 7000, were acquired for each sample (as specified in figure caption). Data were analyzed using the FlowJo software (Tree Star, USA).

Hemolysis assay

The hemolytic activity of quartz particles refers to a method described by Lu & coworkers [67], with minor modifications given by Pavan & coworkers [27]. RBCs were separated from fresh human blood of healthy volunteer donors, not receiving any pharmacological treatment. To assess the effect of FBS proteins on quartz hemolytic activity, particles were incubated with increasing concentration of FBS (0.03%, 0.06%,

0.3%) in the exposure medium (DPBS). Briefly, quartz suspensions (75 µl/well,) at a concentration of 0.37 mg/ml were dispensed in a transparent 96-well Cellstar microplate (Greiner Bio-One, Kremsmunster, Austria), and FBS (75 µl/well) was added, to each well. After 30 minutes of incubation at room temperature (25 °C), red blood cells suspension (75 µl/well) was added, and the plate, gently shaken on an orbital plate shaker, was incubated for 30 minutes at 25 °C.

The plate was centrifuged for 5 minutes at 1200 RPM, using a Centrifuge Rotina 420R centrifuge (Hettic Instruments, Beverly, MA, USA). The supernatant (75 µl) was removed and transferred to a clean transparent microplate. The amount of haemoglobin released into the supernatant was spectrophotometrically determined at a wavelength of 540 nm with an Infinite 200 UV/Vis spectrophotometer (Tecan, Grödig, Austria). Absorbance values were converted into percentages of haemolysis according to the formula (**Equation 1**):

$$\%\,Hemolysis = \frac{(Sample\ OD - Negative\ Control\ Average\ OD)}{(Positive\ Control\ Average\ OD - Negative\ Control\ Average\ OD)} x100 \qquad (1)$$

where OD is the optical density or absorbance.

DPBS and 0.1% Triton-X100 were used as negative and positive controls, respectively. Released hemoglobyn did not adsorbed on quartz samples (data not shown).

Statistical analysis

Statistical analysis was carried out by one-way analysis of variance (ANOVA) followed by Tukey's *post hoc* test, as appropriate. Differences with p value < 0.05 were considered statistically significant.

Abbreviations

AM: alveolar macrophages

AOP: adverse outcome pathway

BET: Brunauer-Emmett-Teller

cRPMI: complete RPMI (RPMI + 10% FBS)

DLS: dynamic light scattering

ELS: electronic light scattering

FBS: fetal bovine serum

FPIA: flow particle image analyser

LMP: lysosome membrane permeabilization

MIE: molecular initiating event

MTT: 3-(4,5-Dimethylthiazol-2-yl)-2,5-Diphenyltetrazolium Bromide

PI: propidium iodide

PMA: phorbol myristyl acetate

RCS: respirable crystalline silica

RPMI: Rosewell Park Memorial Institute 1640 Medium

sfRPMI: serum-free RPMI

SEM: scanning electron microscopy

SSA: specific surface area

TEM: transmission electron microscopy

Declarations

Ethics approval and consent to participate

Not applicable.

Consent for publication

Not applicable.

Availability of data and material

The datasets generated and/or analysed during the current study available from the corresponding author on reasonable request.

Competing interests

The authors declare that they have no competing interests.

Funding

Funding for this project was received from the European Association of Silica Producers (EUROSIL) to RL, CP, MT, and FT, and from H2020-MSCA-COFUND-2015 project ALERT (Grant Agreement number: 713482) to HY and AS.

Authors' contributions

RL designed and carried out the experiments, under the supervision of AS at the University of Groningen, and wrote the manuscript. CP synthesized quartz crystals, performed part of physico-chemical characterization, and carried out hemolysis assay. HY carried out the TEM imaging on fixed cells. MT performed part of physico-chemical characterization. AS designed the cell experiments, interpreted the data and wrote the manuscript. FT supervised the whole project, interpreted the data and wrote the manuscript. All authors read and approved the final manuscript.

Acknowledgements

We kindly thank Prof. Dominique Lison (LTAP, Université catholique de Louvain, Belgium) for fruitful discussion that largely improved the manuscript. Transmission electron microscopy has been performed in the UMCG Microscopy and Imaging Center (UMIC).

References

1. International Agency for Research on Cancer (IARC). **Silica dust, crystalline, in the form of quartz or cristobalite**. IARC Monogr Eval Carcinog Risks to Humans. 2011.
2. **Adverse effects of crystalline silica exposure.** Am. J. Respir. Crit. Care Med. 1997;155:761-8.
3. Parks CG, Conrad K, Cooper GS. **Occupational exposure to crystalline silica and autoimmune disease.** Environ Health Perspect. 1999;107:739-802.
4. Fenoglio I, Fubini B, Tiozzo R, Di Renzo F. **Effect of micromorphology and surface reactivity of several unusual forms of crystalline silica on the toxicity to a monocyte-macrophage tumor cell line.** Inhal Toxicol. 2000;12:81–9.
5. Wiessner JH, Mandel NS, Sohnle PG, Mandel GS. **Effect of Particle Size on Quartz-Induced Hemolysis and on Lung Inflammation and Fibrosis.** Exp Lung Res. 1989;15:801–12.
6. Dalal NS, Shi XL, Vallyathan V. **ESR spin trapping and cytotoxicity investigations of freshly fractured quartz: mechanism of acute silicosis.** Free Radic Res Commun. 1990;9:259–66.
7. Schins RPF, Knaapen AM, Cakmak GD, Shi T, Weishaupt C, Borm PJA. **Oxidant-induced DNA damage by quartz in alveolar epithelial cells.** Mutat Res - Genet Toxicol Environ Mutagen. 2002;517:77–86.
8. Vallyathan V, Shi XL, Dalal NS, Irr W, Castranova V. **Generation of free radicals from freshly fractured silica dust. Potential role in acute silica-induced lung injury.** Am Rev Respir Dis. 1988;138:1213–9.
9. Bolis V, Fubini B, Marchese L, Martra G, Costa D. **Hydrophilic and hydrophobic sites on dehydrated crystalline and amorphous silicas.** J Chem Soc Faraday Trans. 1991;87:497.
10. Hemenway D, Absher A, Fubini B, Trombley L, Vacek P, Volante M, Cavenago A. **Surface functionalities are related to biological response and transport of crystalline silica.** Ann Occup Hyg. 1994;38:447–54.
11. Warheit DB, Webb TR, Colvin VL, Reed KL, Sayes CM. **Pulmonary bioassay studies with nanoscale and fine-quartz particles in rats: Toxicity is not dependent upon particle size but on surface characteristics.** Toxicol Sci. 2007;95:270-80.

12. Gilberti RM, Joshi GN, Knecht DA. **The phagocytosis of crystalline silica particles by macrophages.** Am J Respir Cell Mol Biol. 2008;39:619–27.
13. Shen HM, Zhang Z, Zhang QF, Ong CN. **Reactive oxygen species and caspase activation mediate silica-induced apoptosis in alveolar macrophages.** Am J Physiol Lung Cell Mol Physiol. 2001;280:L10-7.
14. Giordano G, van den Brûle S, Lo Re S, Triqueneaux P, Uwambayinema F, Yakoub Y, Couillin I, Ryffel B, Michiels T, Renauld JC, Lison D, Huaux F. **Type I interferon signaling contributes to chronic inflammation in a murine model of silicosis.** Toxicol Sci. 2010;116:682–92.
15. Pavan C, Fubini B. **Unveiling the Variability of "Quartz Hazard" in Light of Recent Toxicological Findings.** Chem Res Toxicol. 2017;30:469–85.
16. Hamilton RF, Thakur SA, Holian A. **Silica binding and toxicity in alveolar macrophages.** Free Radic. Biol. Med. 2008;44:1246-58.
17. Joshi GN, Goetjen AM, Knecht DA. **Silica particles cause NADPH oxidase-independent ROS generation and transient phagolysosomal leakage.** Mol Biol Cell. 2015;26:3150-64.
18. Rejman J, Oberle V, Zuhorn IS, Hoekstra D. **Size-dependent internalization of particles via the pathways of clathrin- and caveolae-mediated endocytosis.** Biochem J. 2004;377:159-69.
19. Nel AE, Mädler L, Velegol D, Xia T, Hoek EMV V, Somasundaran P, Klaessig F, Castranova V, Thompson M. **Understanding biophysicochemical interactions at the nano-bio interface.** Nat Mater. 2009;8:543–57.
20. Salvati A, Åberg C, dos Santos T, Varela J, Pinto P, Lynch I, Dawson KA. **Experimental and theoretical comparison of intracellular import of polymeric nanoparticles and small molecules: Toward models of uptake kinetics.** Nanomedicine Nanotechnology, Biol Med. 2011;7:818-26.
21. Wang F, Yu L, Monopoli MP, Sandin P, Mahon E, Salvati A, Dawson KA. **The biomolecular corona is retained during nanoparticle uptake and protects the cells from the damage induced by cationic nanoparticles until degraded in the lysosomes.** Nanomedicine Nanotechnology, Biol Med. 2013;9:1159–68.
22. Sabella S, Carney RP, Brunetti V, Malvindi MA, Al-Juffali N, Vecchio G, Janes SM, Bakr OM, Cingolani R, Stellacci F, Pompa PP. **A general mechanism for intracellular toxicity of metal-containing nanoparticles.** Nanoscale. 2014;6:7052-61.
23. Hughes CS, Colhoun LM, Bains BK, Kilgour JD, Burden RE, Burrows JF, Lavelle EC, Gilmore BF, Scott CJ. **Extracellular cathepsin S and intracellular caspase 1 activation are surrogate biomarkers of particulate-induced lysosomal disruption in macrophages.** Part Fibre Toxicol. 2015;13:19.
24. Sayan M, Mossman BT. **The NLRP3 inflammasome in pathogenic particle and fibre-associated lung inflammation and diseases.** Part Fibre Toxicol. 2015;13:51.
25. Rabolli V, Lison D, Huaux F. **The complex cascade of cellular events governing inflammasome activation and IL-1β processing in response to inhaled particles.** Part Fibre Toxicol. 2015;13:40.
26. Pavan C, Rabolli V, Tomatis M, Fubini B, Lison D. **Why does the hemolytic activity of silica predict its pro-inflammatory activity?** Part Fibre Toxicol. 2014;11:76.

27. Pavan C, Tomatis M, Ghiazza M, Rabolli V, Bolis V, Lison D, Fubini B. **In search of the chemical basis of the hemolytic potential of silicas.** Chem Res Toxicol. 2013;26:1188–98.
28. Turci F, Pavan C, Leinardi R, Tomatis M, Pastero L, Garry D, Anguissola S, Lison D, Fubini B. **Revisiting the paradigm of silica pathogenicity with synthetic quartz crystals: the role of crystallinity and surface disorder**. Part Fibre Toxicol. 2016;13:32.
29. Pavan C, Turci F, Tomatis M, Ghiazza M, Lison D, Fubini B. **Z potential evidences silanol heterogeneity induced by metal contaminants at the quartz surface: Implications in membrane damage.** Colloids Surfaces B Biointerfaces. 2017;157:449-455.
30. Nolan RP, Langer AM, Harington JS, Oster G, Selikoff IJ. **Quartz hemolysis as related to its surface functionalities.** Environ Res. 1981;26:503–20.
31. Gerashchenko BI, Gun'ko VM, Gerashchenko II, Mironyuk IF, Leboda R, Hosoya H. **Probing the silica surfaces by red blood cells.** Cytometry. 2002;49:56–61.
32. Zhao Y, Sun X, Zhang G, Trewyn BG, Slowing II, Lin VS. **Interaction of mesoporous silica nanoparticles with human red blood cell membranes: size and surface effects.** ACS Nano. 2011;5:1366–75.
33. Daniel LN, Mao Y, Wang TC, Markey CJ, Markey SP, Shi X, Saffiotti U. **DNA strand breakage, thymine glycol production, and hydroxyl radical generation induced by different samples of crystalline silica in vitro.** Env Res. 1995;71:60–73.
34. Duffin R, Gilmour PS, Schins RP, Clouter A, Guy K, Brown DM, MacNee W, Borm PJ, Donaldson K, Stone V. **Aluminium lactate treatment of DQ12 quartz inhibits its ability to cause inflammation, chemokine expression, and nuclear factor-kappaB activation.** Toxicol Appl Pharmacol. 2001;176:10–7.
35. Fubini B, Hubbard A. **Reactive oxygen species (ROS) and reactive nitrogen species (RNS) generation by silica in inflammation and fibrosis.** Free Radic. Biol. Med. 2003;34:1507-16.
36. Pastero L, Turci F, Leinardi R, Pavan C, Monopoli M. **Synthesis of α-Quartz with Controlled Properties for the Investigation of the Molecular Determinants in Silica Toxicology.** Cryst Growth Des. American Chemical Society; 2016;16:2394–403.
37. Allison AC. **An examination of the cytotoxic effects of silica on macrophages.** J Exp Med. 1966;124:141–54.
38. Castranova V. **Signaling pathways controlling the production of inflammatory mediators in response to crystalline silica exposure: role of reactive oxygen/nitrogen species.** Free Radic Biol Med. 2004;37:916–25.
39. Lison D, Laloy J, Corazzari I, Muller J, Rabolli V, Panin N, Huaux F, Fenoglio I, Fubini B. **Sintered Indium-Tin-Oxide (ITO) particles: A new pneumotoxic entity.** Toxicol Sci. 2009;108:472-81.
40. Pfau JC, Seib T, Overocker JJ, Roe J, Ferro AS. **Functional expression of system x(c)- is upregulated by asbestos but not crystalline silica in murine macrophages.** Inhal Toxicol. 2012;24:476-85.
41. Wottrich R, Diabaté S, Krug HF. **Biological effects of ultrafine model particles in human macrophages and epithelial cells in mono- and co-culture.** Int J Hyg Environ Health. 2004;207:353-61.

42. Theus SA, Cave MD, Eisenach KD. **Activated THP-1 cells: an attractive model for the assessment of intracellular growth rates of Mycobacterium tuberculosis isolates.** Infect Immun. 2004;72:1169-73.
43. Kletting S, Barthold S, Repnik U, Griffiths G, Loretz B, Schneider-Daum N, de Souza Carvalho-Wodarz C, Lehr CM. **Co-culture of human alveolar epithelial (hAELVi) and macrophage (THP-1) cell lines.** ALTEX. 2018;35:211-222.
44. Thibodeau MS, Giardina C, Knecht DA, Helble J, Hubbard AK. **Silica-induced apoptosis in mouse alveolar macrophages is initiated by lysosomal enzyme activity.** Toxicol Sci. 2004;80:34-48.
45. Hornung V, Bauernfeind F, Halle A, Samstad EO, Kono H, Rock KL, Fitzgerald KA, Latz E. **Silica crystals and aluminum salts activate the NALP3 inflammasome through phagosomal destabilization.** Nat Immunol. 2008;9:847–56.
46. Dostert C, Pétrilli V, Van Bruggen R, Steele C, Mossman BT, Tschopp J. **Innate immune activation through Nalp3 inflammasome sensing of asbestos and silica.** Science. 2008;320:674-7.
47. Sellamuthu R. **Blood gene expression profiling detects silica exposure and toxicity.** Toxicol Sci. 2011;122:253–64.
48. Murashov V V., Demchuk E. **A comparative study of unrelaxed surfaces on quartz and kaolinite, using the periodic density functional theory.** J Phys Chem B. 2005;109:10835–41.
49. Turci F, Ghibaudi E, Colonna M, Boscolo B, Fenoglio I, Fubini B. **An integrated approach to the study of the interaction between proteins and nanoparticles.** Langmuir. 2010;26:8336-46.
50. Wang F, Salvati A, Boya P. **Lysosome-dependent cell death and deregulated autophagy induced by amine-modified polystyrene nanoparticles.** Open Biol. 2018;8(4).
51. Latz E, Xiao TS, Stutz A. **Activation and regulation of the inflammasomes.** Nat. Rev. Immunol. 2013;13:397-411.
52. Sharma D, Kanneganti TD. **The cell biology of inflammasomes: Mechanisms of inflammasome activation and regulation.** J. Cell Biol. 2016. p. 617–29.
53. Mossman BT, Churg A. **Mechanisms in the pathogenesis of asbestosis and silicosis.** Am J Respir Crit Care Med. 1998;157:1666–80.
54. Albrecht C, Höhr D, Haberzettl P, Becker A, Borm PJA, Schins RPF. **Surface-dependent quartz uptake by macrophages: potential role in pulmonary inflammation and lung clearance**. Inhal Toxicol. 2007;19:39–48.
55. Cassel SL, Eisenbarth SC, Iyer SS, Sadler JJ, Colegio OR, Tephly LA, Carter AB, Rothman PB, Flavell RA, Sutterwala FS. **The Nalp3 inflammasome is essential for the development of silicosis.** Proc Natl Acad Sci. 2008;105:9035–40.
56. Bernstein D, Castranova V, Donaldson K, Fubini B, Hadley J, Hesterberg T, Kane A, Lai D, McConnell EE, Muhle H, Oberdorster G, Olin S, Warheit DB. **Testing of fibrous particles: Short-term assays and strategies** - Report of an ILSI Risk Science Institute Working Group. Inhal. Toxicol. 2005;17:497-537.
57. Peeters PM, Eurlings IMJ, Perkins TN, Wouters EF, Schins RPF, Borm PJ, Drommer W, Reynaert NL, Albrecht C. **Silica-induced NLRP3 inflammasome activation in vitro and in rat lungs.** Part Fibre

Toxicol. 2014;11:58.

58. Ziemann C, Escrig A, Bonvicini G, Ibáñez MJ, Monfort E, Salomoni A, Creutzenberg O. **Organosilane-based coating of quartz species from the traditional ceramics industry: Evidence of hazard reduction using in vitro and in vivo tests.** Ann Work Expo Heal. 2017;61:468-480.
59. He Y, Hara H, Núñez G. **Mechanism and Regulation of NLRP3 Inflammasome Activation.** Trends Biochem. Sci. 2016;41:1012-1021.
60. Pavan C, Delle Piane M, Gullo M, Filippi F, Fubini B, Hoet P, Horwell CJ, Huaux F, Lison D, Lo Giudice C, Martra G, Montfort E, Schins R, Sulpizi M, Wegner K, Wyart-Remy M, Ziemann C, Turci F. **The puzzling issue of silica toxicity: are silanols bridging the gaps between surface states and pathogenicity?** Part Fibre Toxicol [Internet]. 2019;16:32.
61. Pavan C, Santalucia R, Leinardi R, Fabbiani M, Yakoub Y, Uwambayinema F, et al. Nearly-free silanols generated by fracturing determine the pathogenic activity of silica particles. *In preparation*.
62. Tsuchiya S, Yamabe M, Yamaguchi Y, Kobayashi Y, Konno T, Tada K. **Establishment and characterization of a human acute monocytic leukemia cell line (THP-1).** Int J cancer. 1980;26:171-6.
63. Tsuchiya S, Gota Y, Okumura H, Nakae S, Konno T, Tada K, et al. **Induction of maturation in cultured human monocytic leukemia cells by a phorbol diester.** Cancer Res. 1982;42:1530-6
64. Gerlier D, Thomasset N. **Use of MTT colorimetric assay to measure cell activation.** J Immunol Methods. 1986;94:57–63.
65. Sharma G, Valenta DT, Altman Y, Harvey S, Xie H, Mitragotri S, Smith JW. **Polymer particle shape independently influences binding and internalization by macrophages.** J Control Release. 2010;147:408-12.
66. Dunn WA, Hubbard AL, Aronson NN. **Low temperature selectively inhibits fusion between pinocytic vesicles and lysosomes during heterophagy of125I-asialofetuin by the perfused rat liver.** J Biol Chem. 1980;255:5971-8.
67. Lu S, Duffin R, Poland C, Daly P, Murphy F, Drost E, Macnee W, Stone V, Donaldson K. **Efficacy of simple short-term in vitro assays for predicting the potential of metal oxide nanoparticles to cause pulmonary inflammation.** Environ Health Perspect. 2009;117:241–7.

Figures

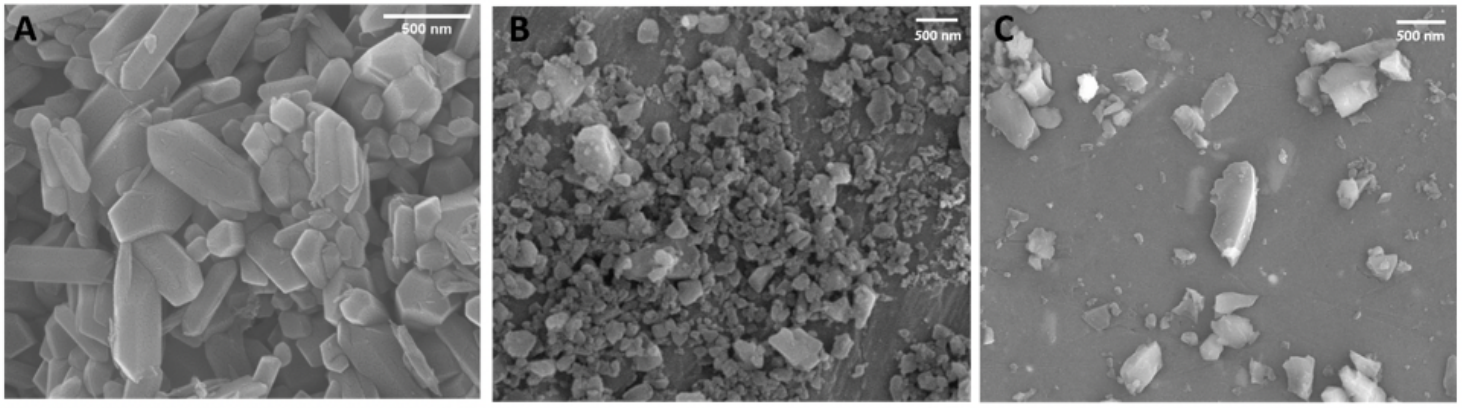

Figure 1

FE-SEM imaging of gQ, gQ-f and cQ-f quartz samples. Synthetic regular quartz crystals (gQ, a) show as-grown, flat and smooth surfaces; fractured quartz crystals (gQ-f and cQ-f, b and c) exhibit irregular surfaces and the typical fractures due to mechanical fracturing

Figure 2

Representative images by transmission electron microscopy (TEM) of differentiated THP-1 human macrophages exposed to quartz particles. Cells were exposed to synthetic as-grown (gQ, c and d) and fractured (gQ-f, e and f) quartz particles (50 µg ml-1) for 24 h. Panels a and b show equivalent images of untreated cells, and g and h show cells exposed to positive control (cQ-f). Electron microscopy confirmed that all types of particles (black arrows) were internalized by macrophages. Scale bars: 10 µm (a, c, e, g), and 1 µm (b, d, f, h)

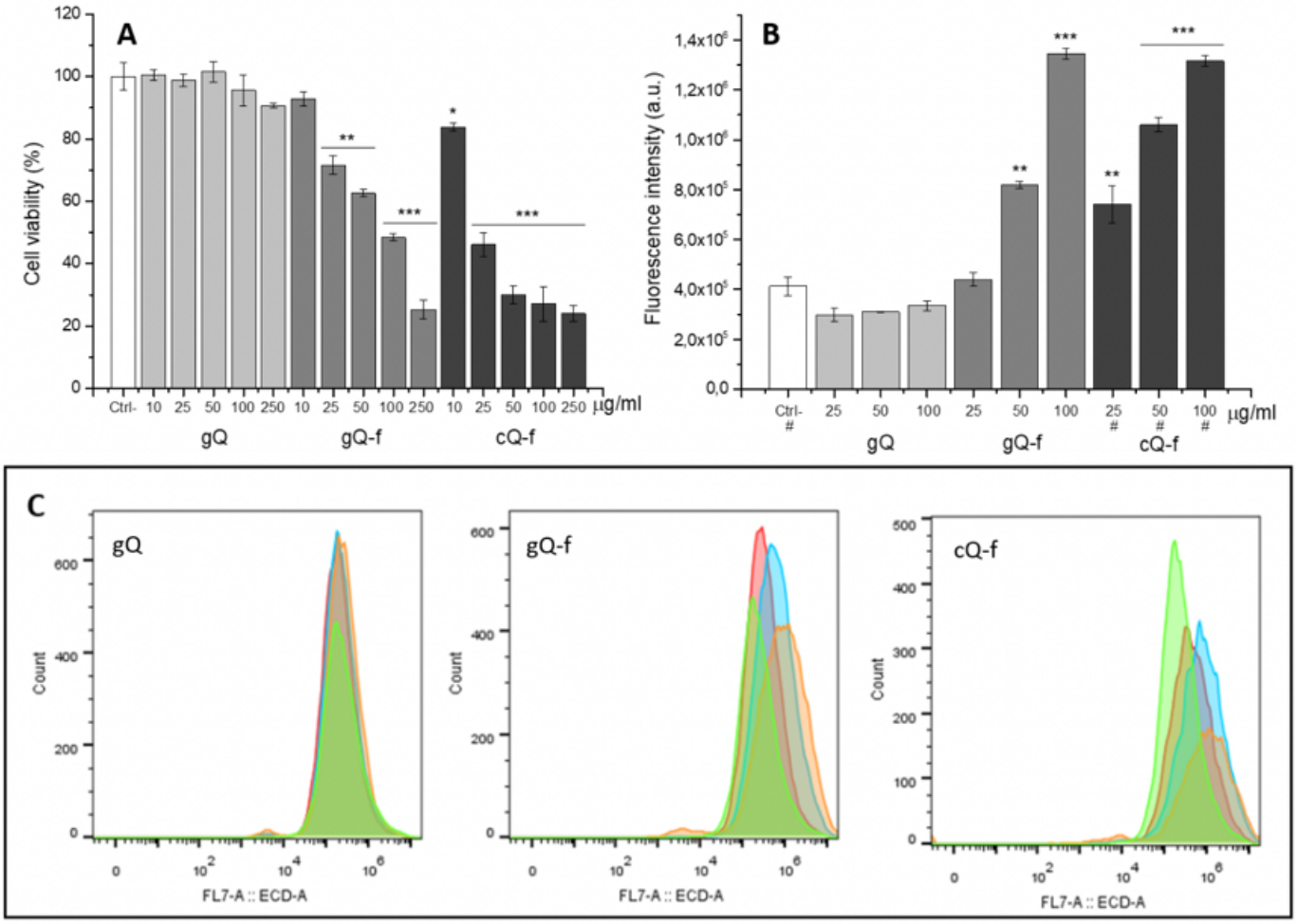

Figure 3

Impact of quartz particles on cell viability and lysosome alteration, after 24h exposure to increasing doses of quartz particles in cRPMI. The cell viability, investigated by MTT assay, is expressed as a percentage with respect to untreated cells (a). The mitochondrial activity significantly decreased only upon exposure to fractured quartz (gQ-f and cQ-f). Data are the mean (±SD) of four biological replicates of one representative experiment out of three. The impact on phagolysosomes was measured by incubation of differentiated THP-1 macrophages with quartz, followed by staining with Lyso Tracker Red dye (b and c). Fluorescence variation was evaluated by flow cytometry: mean fluorescence (b) and corresponding Lyso Tracker intensity distributions (c). Quartz concentrations are identified by the colour code described as follows (c): red: 25 □g ml-1; cyan: 50 □g ml-1; orange: 100 □g ml-1; green: untreated cells. The Lyso Tracker Red data shown is the result of three biological replicates of one representative experiment out of three. Cell counts ranged from ca. 7600 to 20000. Concentrations where less than 20000 cells were counted, are highlighted by a hash mark (#). For synthetic quartz samples (gQ and gQ-f), 20000 cells were counted on average, for each dosage. Because of cytotoxicity, fewer cells were counted for cQ-f (25 □g ml-1: 12728 cells; 50 □g ml-1: 13575 cells: 100 □g ml-1: 7680 cells). Untreated cells ranged from 16300 to 18500. Differences between negative control and quartz-exposed cells were

evaluated with one-way ANOVA, followed by Tukey's post-hoc analysis. p-values < 0.05 were considered statistically significant. * p <0.05, ** p <0.01, *** p <0.001 vs. control not exposed to quartz.)

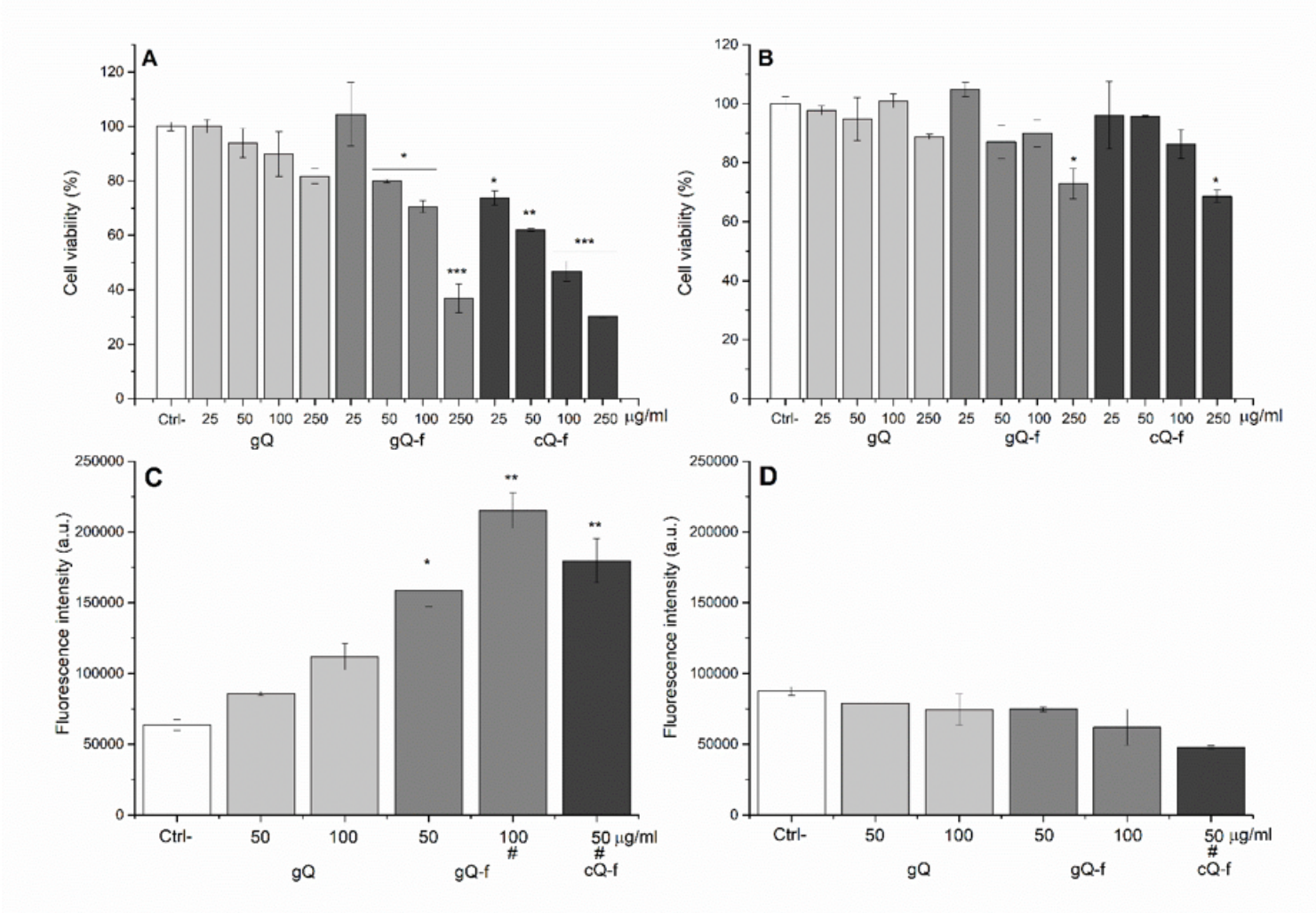

Figure 4

Macrophages exposure to quartz particles in energy depleted conditions. PMA-differentiated THP-1 macrophages were exposed for 4 h to increasing doses of quartz particles in cRPMI, in standard (a and c) or energy depleted (b and d) conditions, followed by particle removal and further incubation at 37°C for 20 h. Impact on cell viability was evaluated via MTT (a and b). Data are from one representative experiment, using four replicates per dose, and are expressed as a percentage with respect to untreated cells. Phagolysosome alteration (c and d) was investigated by staining cells with Lyso Tracker Red dye, and flow cytometry. Data are the mean (± SD) of one representative experiment, with two replicates for each condition. Counted cells ranged from ca. 15000 to 20000. Concentrations where less than 20000 cells were counted are highlighted by a hash mark (#). Differences between negative control and quartz-exposed cells were evaluated with one-way ANOVA, followed by Tukey's post-hoc analysis. p-values < 0.05 were considered statistically significant. * p <0.05, ** p <0.01, *** p <0.001 vs. control not exposed to quartz.)

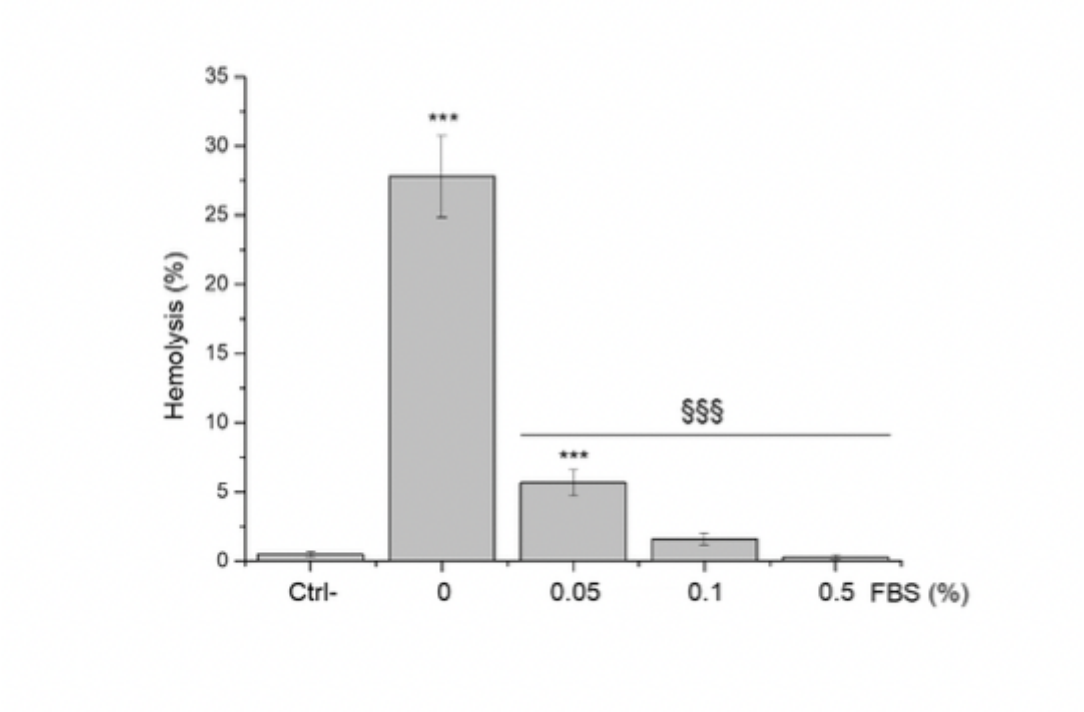

Figure 5

Hemolytic activity of gQ-f in absence or presence of FBS. Synthetic fractured quartz was incubated 30 minutes at 25°C with purified human red blood cells, in the presence of increasing concentrations of FBS (0, 0.05, 0.1 and 0.5%). FBS was not removed during RBCs exposure to particles. Dispersion in medium with protein reduced the hemolytic activity of quartz particles. Data were analysed with one-way ANOVA, followed by Tukey's post-hoc analysis. p-values < 0.05 were considered statistically significant. * p <0.05, ** p <0.01, *** p <0.001 vs. control not exposed to quartz. § p <0.05, §§ p <0.01, §§§ p <0.001 vs. hemolysis with no FBS (0% FBS)

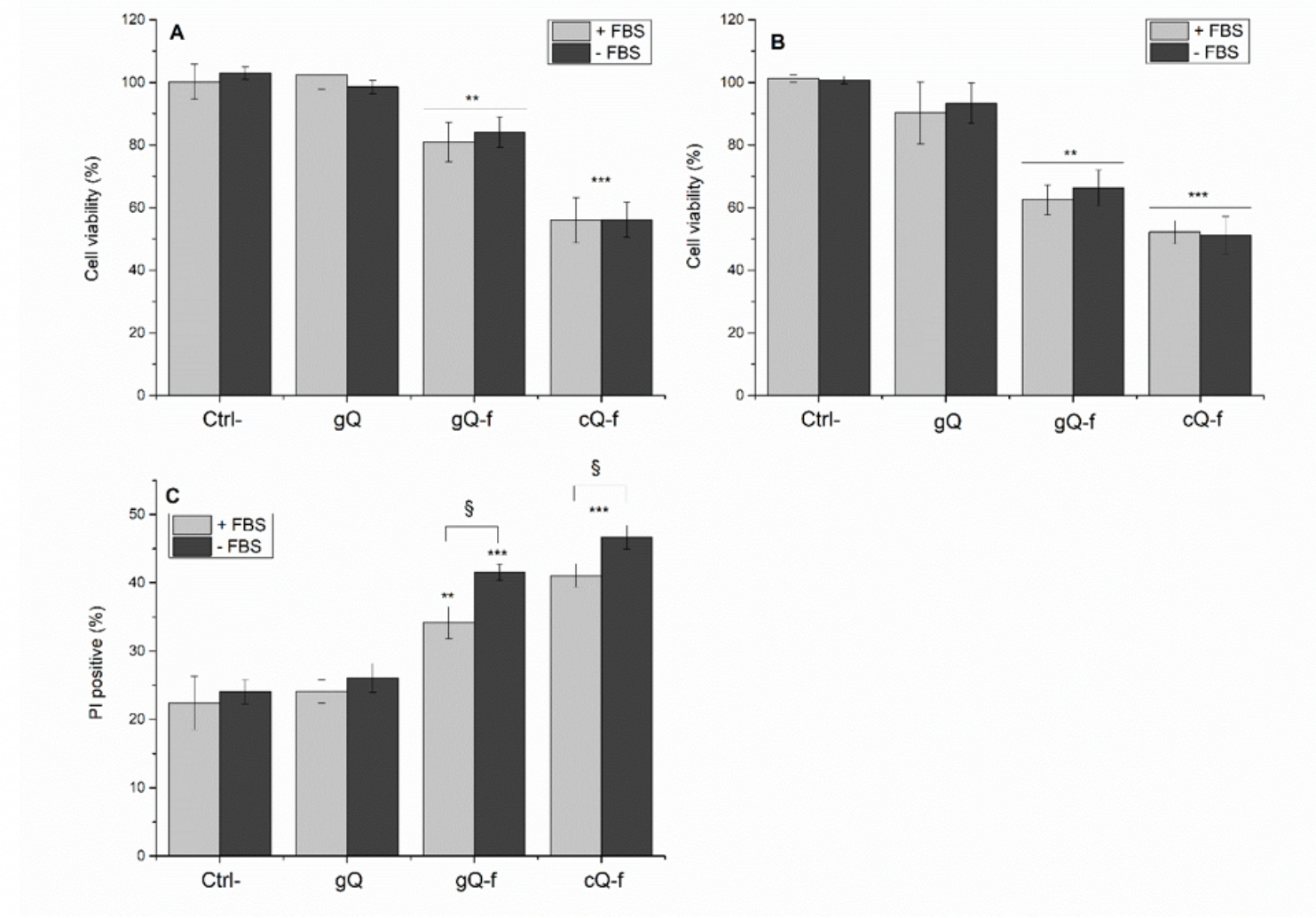

Figure 6

Impact of FBS on quartz cytotoxicity. The effect of FBS on quartz cytotoxicity was evaluated via MTT assay after 4 and 24 h exposure (a and b, respectively), and % of PI-positive cells (c), as measured by staining with propidium iodide and flow cytometry (4 h exposure). THP-1 macrophages were exposed to particles (100 □g/ml) in presence of 10% FBS (+ FBS) or in serum-free RPMI (- FBS). Cytotoxicity is observed for fractured samples only, as expected. Comparing + FBS and - FBS exposures, MTT readouts at both 4 (a) and 24 h (b) were similar, while PI assay (c) showed small differences for fractured particles only. MTT data are from one representative experiment out of three, using four replicate wells per concentration, and are expressed as a percentage with respect to the values of untreated cells. PI assay data result from one representative experiment, using four replicates. A variable number of cells ranging from a minimum of ca. 7000 (cQ-f) to a maximum of ca. 12000 (gQ) were counted. Data are expressed as means (±SD). Differences between negative control and quartz exposed-cells and + FBS vs. - FBS were evaluated with one-way ANOVA, followed by Tukey's post-hoc analysis. p-values < 0.05 were considered

statistically significant. * p <0.05, ** p <0.01, *** p <0.001 vs. control not exposed to quartz. § p <0.05, §§ p <0.01, §§§ p <0.001 for + FBS vs. - FBS.)